Wrapping conformations of a polymer on a curved surface

Cheng-Hsiao Lin,[1,2] Yan-Chr Tsai,[1,*] and Chin-Kun Hu[2,†]

[1]*National Chung-Cheng University, Chia-Yi 621, Taiwan*
[2]*Institute of Physics Academia Sinica, Nankang, Taipei 11529, Taiwan*

The conformation of a polymer on a curved surface is high on the agenda for polymer science. We assume that the free energy of the system is the sum of bending energy of the polymer and the electrostatic attraction between the polymer and surface. As is also assumed, the polymer is very stiff with an invariant length for each segment so that we can neglect its tensile energy and view its length as a constant. Based on the principle of minimization of free energy, we apply a variation method with a locally undetermined Lagrange multiplier to obtain a set of equations for the polymer conformation in terms of local geometrical quantities. We have obtained some numerical solutions for the conformations of the polymer chain on cylindrical and ellipsoidal surfaces. With some boundary conditions, we find that the free energy profiles of polymer chains behave differently and depend on the geometry of the surface for both cases. In the former case, the free energy of each segment distributes within a narrower range and its value per unit length oscillates almost periodically in the azimuthal angle. However, in the latter case the free energy distributes in a wider range with larger value at both ends and smaller value in the middle of the chain. The structure of a polymer wrapping around an ellipsoidal surface is apt to dewrap a polymer from the endpoints. The dependence of threshold lengths for a polymer on the initially anchored positions is also investigated. With initial conditions, the threshold wrapping length is found to increase with the electrostatic attraction strength for the ellipsoidal surface case. When a polymer wraps around a sphere surface, the threshold length increases monotonically with the radius without the self-intersection configuration for a polymer. We also discuss potential applications of the present theory to DNA/protein complex and further researches on DNA on the curved surface.

PACS number(s): 87.15.−v, 87.14.Gg, 68.43.De, 21.45.+v

I. INTRODUCTION

The conformation of a polymer on a curved surface is a fundamental issue in polymer science which is related to some important biological processes and technological applications. In particular, polymer wrapping is relevant to DNA packaging in cells, where the genomic DNA is compactly folded onto chromatins through several hierarchical steps [1].

The theoretical understanding of the supercoiled configurations of plasmids has been obtained by modeling a DNA as a wormlike chain (WLC) characterized by the bending and twisting (torsional) rigidities [2,3]. The elastic properties of a DNA chain greatly influence (or regulate) its biological functions [4]. In a host of biological processes, such as packaging, transcription, regulation and repair, different parts of a DNA molecule should collaborate with each other by flexibility of the DNA chain.

A polyelectrolyte (PE) absorbing on colloid particles or micelles, and a DNA binding to latex particles and dendrimers, which were also under intensive investigations recently [5,6]. A negatively charged DNA chain, a PE, will be held to the protein core with oppositely charged lysines or arginines against its tendency to straighten if the DNA/protein complex attractive interactions are sufficiently strong. The DNA/protein complex will dissociate if their mutual attractive forces are weakened, where a DNA unwraps the protein core.

Experiments show that the binding strength of a PE varies with several parameters, such as temperature, salt concentration, surface charge density, and linear charge density of the PE. This attractive strength will govern wrapping-unwrapping phase transition [7]. The polymer statistics on curved surfaces have also been investigated [8,9]. However, the conformation of a WLC wrapping around a curved surface is seldom addressed and is still an open question. To investigate the conformation of a WLC folded onto a curved surface, we consider a simplified model. We assume that the free energy of the system is the sum of bending energy of the polymer and the electrostatic attraction between the polymer and surface. We also assume that the polymer is very stiff with an invariant length for each segment so that we can neglect its strain energy and view its length as a constant. Based on the principle of minimization of free energy and with the aid of differential geometry, we can derive a set of differential equations to determine the shape of a polymer meandering on a given curved surface.

This paper is organized as follows. In Sec. II we first propose a simplified model for the polymer energy. Based on the principle of minimization of free energy, we derive a set of coupled nonlinear differential equations for a specific conformation of a polymer chain on the curved surface with given boundary conditions. In Sec. III we present numerical solutions with boundary and initial conditions for the conformations of the polymer on cylindrical and ellipsoidal surfaces. Finally, in Sec. IV we summarize our numerical results and discuss issues for further studies. For illustrating the validity of the mathematical method used in Sec. II we take the classic geodesic problem as an example in Appendix A. More detailed derivation of the set of coupled nonlinear dif-

*Corresponding author; Electronic address: tyan@phy.ccu.edu.tw
†Electronic address: huck@phys.sinica.edu.tw

ferential equations for a specific conformation of a WLC on a curved surface is presented in Appendix B. In Appendix C, we will demonstrate to derive a set of coupled differential equations for specific conformation of a WLC including the torsional energy effect for academic interest.

II. THEORETICAL MODEL

In our simplified model, the electrostatic interactions between segments and polymer chain extensibility are neglected, which is a trade-off between computational efforts and physical rigor. In the appreciated WLC model [2], the elastic energy of a chain with contour length L is given by the sum of the bending energy H_{ben}, the twisting energy H_{tw} [2], and the electrostatic attraction energy H_{att} between the chain and the surface. The shape of a WLC will be determined by the competition between the elastic energy and the attraction energy. For the polymers with helix structure will contain a twisting energy [10]. For simplicity, we consider the case of a WLC with a small twisting rate and its twisting energy can be neglected or the cases of polymers without helix structure. In the coarse-grain sense, the outer of a spool will be approximated as a smooth surface. In the WLC model, the total system free energy is given as usual by [10]

$$H_{\text{tot}} = H_{\text{ben}} + H_{\text{att}}, \tag{1}$$

where

$$H_{\text{ben}} = \frac{A}{2} \int_0^L \kappa^2(s)ds, \tag{2}$$

$$H_{\text{att}} = D \int_0^L ds \tag{3}$$

(ds denotes the arc-length element of the chain); $\kappa(s)$ corresponds to curvature of the chain at the point parametrized by the arc-length s and A denotes elastic rigidity. In the case of DNA/protein complex, typical value of A is $50k_BT \cdot$nm with k_B being the Boltzmann constant and T the environment temperature [3,11]. The value of D is the order of $-k_BT/b_0$ with b_0 the spacing between charges along the chain [10] and its value is about $-1 \sim -10k_BT/$nm for a DNA-protein complex. One should note in passing that the value of A and D are temperature dependent. We assume that each segment of a chain is inextensible [12]. Thus the WLC length remains fixed and will be left as a constraint in our approach. A principal assumption in this paper is that, each segment of the WLC can lie on the surface due to their sufficiently strong attractions [10]. We expect the WLC meandering on a curved surface will adjust its chain conformation such that the system energy assumes the minimum, based on which differential equations determining the conformation of a WLC wrapping around a curved surface can be obtained.

Before deriving the governing equations, we first introduce related notations. Each point of a space curve is determined by its position vector $\mathbf{r} = \mathbf{r}(s)$ where s is a scalar parameter associated with the point along the curve and is taken to be the arc-length here for it is a reparametrization

invariant. The unit tangent vector at a point s is defined as

$$\mathbf{T}(s) = \frac{d\mathbf{r}(s)}{ds}, \tag{4}$$

and its derivative takes the form of

$$\frac{d\mathbf{T}(s)}{ds} = \kappa(s)\mathbf{N}(s), \tag{5}$$

where

$$\mathbf{N}(s) = \frac{d^2\mathbf{r}(s)}{ds^2} \bigg/ \left| \frac{d^2\mathbf{r}(s)}{ds^2} \right| \tag{6}$$

is the principal normal vector. As mention above, $\kappa(s)$ is the curvature of a space curve at s.

A curve lying on a curved surface can be characterized by the curvature vector $\kappa(s)\mathbf{N}(s)$ which can be decomposed into two orthogonal components as follows: the coefficient of one lying on the tangent plane is the so-called geodesic curvature $\kappa_g(s)$ and that of the other one in the positive normal direction of the tangent plane the normal curvature $\kappa_n(s)$. They are related by the equation [13]

$$\kappa(s)\mathbf{N}(s) = \kappa_g(s)[\mathbf{n}(s) \times \mathbf{T}(s)] + \kappa_n(s)\mathbf{n}(s), \tag{7}$$

where $\mathbf{n}(s)$ is the unit normal vector perpendicular to the tangent plane at the point $\mathbf{r}(s)$.

To study the boundary value problem, we consider a family of curves with two fixed endpoints, parametrized as

$$C_\lambda : \mathbf{r}(s, \lambda) = \mathbf{r}(u_1(s, \lambda), u_2(s, \lambda)), \tag{8}$$

where each curve is specified by the parameter λ. A WLC meandering along the curve C_λ with its free energy assuming a minimum corresponds to the conformation C_0. We define the variation of $\mathbf{r}(s, \lambda)$ with respect to λ at $\lambda = 0$ with the fixed s as

$$\mathbf{J}(s) \equiv \left. \frac{\partial \mathbf{r}(u_1(s, \lambda), u_2(s, \lambda))}{\partial \lambda} \right|_{\lambda=0}. \tag{9}$$

Note that the vector function $\mathbf{J}(s)$ at the initial and terminal points assumes zero vectors. The vector $\mathbf{J}(s)$ lying on the tangent plane of the curved surface can be decomposed into [13]

$$\mathbf{J}(s) = l(s)\mathbf{T}(\mathbf{s}) + h(s)\mathbf{n}(s) \times \mathbf{T}(s), \tag{10}$$

where $\mathbf{n}(s)$ and $\mathbf{T}(s)$ are unit normal vector of the curved surface and the tangent vector of curve C_0 at s, respectively. In addition, $\mathbf{J}(s)$ is presumably a smooth vector function on the curved surface and $l(s)$ and $h(s)$ are two arbitrary functions with certain conditions imposed.

Under the constraint of the constant length for each segment, or $|\partial \mathbf{r}(s, \lambda)/\partial s|ds =$ constant, the Euler equation can be written as

$$\frac{\partial H_{\text{tot}}}{\partial \lambda} + \sum \gamma(s) \left. \frac{\partial f(s, \lambda)}{\partial \lambda} \right|_{\lambda=0} = 0, \tag{11}$$

where

$$f(s,\lambda) = \left| \frac{\partial \mathbf{r}(s,\lambda)}{\partial s} \right| ds - \Delta L = 0 \qquad (12)$$

and $\gamma(s)$ is a locally undetermined Lagrange multiplier. With the help of Eqs. (4) and (9), the constraint term in Eq. (11) can be written as

$$\lim_{\Delta L \to 0} \sum \gamma(s) \frac{\partial f(s,\lambda)}{\partial \lambda} \Bigg|_{\lambda=0}$$

$$= \int_{C_\lambda} \gamma(s) \frac{\partial}{\partial \lambda} \sqrt{\frac{\partial \mathbf{r}(s,\lambda)}{\partial s} \frac{\partial \mathbf{r}(s,\lambda)}{\partial s}} ds \Bigg|_{\lambda=0}$$

$$= \int_0^L \gamma(s) \mathbf{J}'(s) \cdot \mathbf{T}(s) ds, \qquad (13)$$

where we have used $\partial^2 \mathbf{r}(s,\lambda) / \partial \lambda \partial s|_{\lambda=0} = \partial[\partial \mathbf{r}(s,\lambda) / \partial \lambda|_{\lambda=0}] / \partial s = \mathbf{J}'(s)$. Here we denote the first and second derivative of a function with respect to s, such as $\mathbf{r}(s)$, as $\mathbf{r}'(s)$ and $\mathbf{r}''(s)$, and its nth order derivative as $\mathbf{r}^{(n)}(s)$ for $n > 2$. The fixed-segment length assumption is valid for the case of DNA not under a large tension (< 65 pN) [14]. On the other hand, the attraction theory for a WLC under a large tension should be modified. But that will result in much more complications for the problem.

To simplify Eq. (13), we substitute Eq. (10) into Eq. (13) and note the same endpoints of C_0 and C_λ will render $l(0) = l(L) = 0$ and $h(0) = h(L) = 0$. It is straightforward to obtain

$$\lim_{\Delta L \to 0} \sum \gamma(s) \frac{\partial f(s,\lambda)}{\partial \lambda} \Bigg|_{\lambda=0} = -\int_0^L l(s) \gamma'(s) ds$$

$$- \int_0^L h(s) \gamma(s) \kappa_g(s) ds. \qquad (14)$$

In a similar way, a straightforward but tedious calculation with additionally imposing conditions $h'(0) = h'(L) = 0$ yields

$$\frac{\partial H_{\text{ben}}}{\partial \lambda} \Bigg|_{\lambda=0} = \frac{A}{2} \int_0^L [l(s)(-8\kappa'(s)\kappa(s)) + h(s)X(s)] ds, \qquad (15)$$

$$\frac{\partial H_{\text{att}}}{\partial \lambda} \Bigg|_{\lambda=0} = -D \int_0^L h(s) \kappa_g(s) ds, \qquad (16)$$

where

$$X(s) = 2\kappa_g \mathbf{n} \cdot \mathbf{n}'' - 3\kappa_g \kappa^2 - 2\kappa_n \mathbf{n}'' \cdot (\mathbf{T} \times \mathbf{n}) + 2\kappa_g''$$

$$- 4\kappa_n' \mathbf{n}' \cdot (\mathbf{T} \times \mathbf{n}) - 4\kappa_n \kappa_g \mathbf{n}' \cdot \mathbf{T}. \qquad (17)$$

Quantities appearing in the above equations, e.g., κ, $\mathbf{T}$, ... and their associated derivatives, are all reparametrization invariants and they are independent of the choice of specific coordinate systems. The reader is referred to Appendix B for the detailed derivations of Eq. (15). Substituting Eqs. (14)–(16) into Eq. (11), we obtain

$$\int_0^L \left[[-\gamma'(s) - 4A\kappa(s)\kappa'(s)] l(s) \right.$$

$$\left. + \left(\frac{A}{2} X(s) - \gamma(s)\kappa_g(s) - D\kappa_g(s) \right) h(s) \right] ds = 0, \quad (18)$$

which is the main result of this paper. Because $l(s)$ and $h(s)$ in Eq. (18) can be treated as independent arbitrary functions after inserting the Lagrange's multiplier $\gamma(s)$, both of their coefficients should be null, i.e., the least-energy conformation should satisfy the following two equations:

$$\gamma'(s) + 4A\kappa(s)\kappa'(s) = 0, \qquad (19)$$

$$\frac{A}{2} X(s) - [\gamma(s) + D]\kappa_g(s) = 0. \qquad (20)$$

The expressions of Eqs. (19) and (20) are reparametrization invariant. Meanwhile, the magnitude of the unit tangent vector should be 1,

$$|\mathbf{r}'(s)|^2 = \sum_{i,j=1}^2 g_{ij} \frac{du_i}{ds} \frac{du_j}{ds} = 1, \qquad (21)$$

where g_{ij} is the metric tensor depending on the shape of a surface. Equation (21) should be viewed as the third equation for determining the WLC conformation. Let $(u_1(s), u_2(s))$ be the coordinates of C_0 on the curved surface, all geometric variables, such as $\kappa(s)$, the metric tensor g_{ij}, etc., can be cast in terms of the variables $(u_1(s), u_2(s))$. Now we are left with three unknown functions, $u_1(s)$, $u_2(s)$, and $\gamma(s)$, and they should be uniquely solved from three coupled highly nonlinear differential equations, i.e., Eqs. (19)–(21), with proper boundary conditions.

Now we turn to the case of only one point of a WLC being initially anchored on the curved surface. The conformation of the full chain is achieved by attaching the segments one by one to the surface (in a unit of a base pair for the DNA case). If the attraction energy is sufficiently large, the chain conformation can maintain under the thermal fluctuations, and therefore the conformation of each segment will be determined by the minimization of its own (segment) total energy. By performing the variation of energy with one endpoint fixed and an infinitesimal small segment length δL, we find the conformation still can be described by the same three equations, Eqs. (19)–(21), which correspond to the initial value problem at the anchored point instead of the boundary value problem. We shall investigate the behaviors of the solutions of Eqs. (19)–(21), with initial or boundary conditions for cylindrical and ellipsoidal surfaces.

III. APPLICATIONS

Cylindrical surface. A cylindrical surface can be parametrized by variables θ and z via the vector function: $\mathbf{r}(\theta,z) = (\rho \cos\theta, \rho \sin\theta, z)$, $0 \le \theta < 2\pi$, $0 \le z \le L_0$, where ρ and L_0 are, respectively, the radius and height of a cylinder. The conformation of a polymer on this surface can be described by $\mathbf{r}(\theta(s), z(s)) = (\rho \cos\theta(s), \rho \sin\theta(s), z(s))$. Then Eq. (21) reduces to
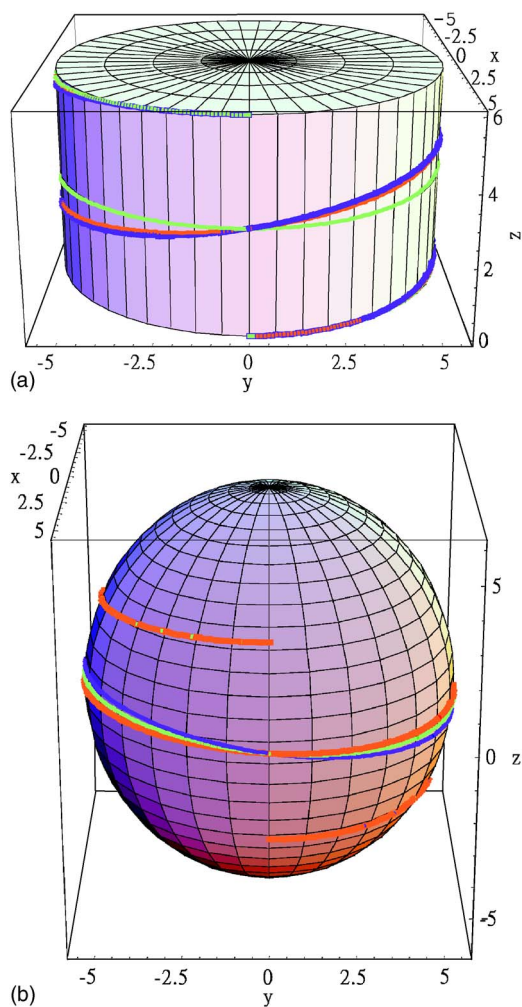
(a)

(b)

FIG. 1. (Color online) Schematics of WLCs wrapping around curved surfaces. (a) WLCs wrapping around a cylindrical surface. (b) WLCs wrapping around an ellipsoidal surface. The boundary conditions in (a) and (b) are the same as those in Figs. 2 and 4, respectively.

$$\rho^2[\theta'(s)]^2 + [z'(s)]^2 = 1. \tag{22}$$

In view of complication and nonlinearity in Eqs. (19), (20), and (22), we can only restore to their numerical solutions. To find the specific boundary-value solutions, we should specify six boundary values of (θ, z), z' at two endpoints, and the length of L in advance. In other words, with a given chain length and position coordinates, slopes of a WLC at its endpoints, its conformation can be obtained by solving the differential equations. In this work, we utilize the shooting method to solve the boundary value problems by the fourth-order Runge-Kutta technique [15] and the relevant parameters are taken for the case of a DNA-protein complex. Here ρ and L_0 are taken as 5.5 and 6 nm, respectively. If not explicitly mentioned, bending stiffness of a WLC, A, and attraction strength D will take the values of $50k_BT \cdot$nm and $-1.2k_BT/$nm, respectively. Figure 1(a) is a schematic picture of the conformation of three WLCs wrapping around a cylindrical surface with the same two endpoints, whose boundary conditions will be presented in the next paragraph.
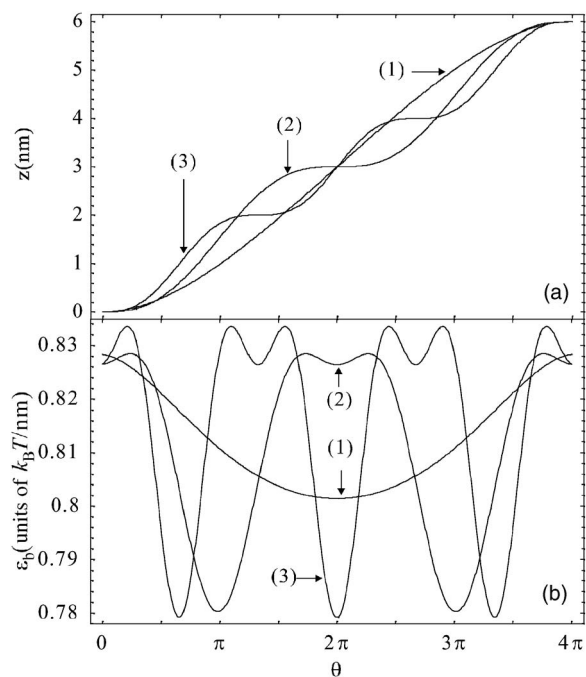

FIG. 2. Conformations of a WLC wrapping around a cylindrical surface with two identical endpoints: (a) Dependence of z on θ, (b) ε_b versus θ. For curves (1), (2), and (3) their boundary conditions are imposed as $(\theta(0), z(0), z'(0)) = (0,0,0)$ and $(\theta(L), z(L), z'(L)) = (4\pi, 6, 0)$, and their lengths are 69.420, 69.498, and 69.501 nm, respectively.

Figure 2(a) shows the dependence of z on θ for three conformations of a WLC wrapping around a cylindrical surface. Here curves (1), (2), and (3) correspond to the red, green, and blue curves in Fig. 1(a), respectively. The coordinates of the two endpoints are $(\theta, z) = (0,0)$ and $(4\pi, 6)$ for $s = 0$ and L, respectively. In Fig. 2 three different conformations are displayed with the same boundary conditions, $z'(0) = z'(L) = 0$, but different contour lengths, where the contour lengths are 69.420, 69.498, and 69.501 nm for curves (1), (2), and (3), respectively. Curves (1), (2), and (3) have 0, 1, and 2 terraces, respectively. It seems there are more terraces formed for longer WLCs.

Figure 2(b) shows the bending energy per unit length versus θ for the three conformations in Fig. 2(a). Here the symbol ε_b stands for the bending energy per unit length. Curves (2) and (3) exhibit approximately periodic oscillations with respect to the coordinate θ and bending energy per unit length ε_b seems to have a tendency to spread over the WLC uniformly. Comparing Figs. 2(a) with 2(b), we find that the positions close to the terrace in Fig. 2(a) correspond to larger bending curvature of WLC and then higher bending energy.

Figure 3 shows ε_b distribution diagram corresponding to Fig. 2(b). Here the total sample number N is equal to 5000 and the interval $\Delta\varepsilon_b$ is equal to $0.005k_BT/$nm. The standard deviations for the data are calculated as 0.009 150 49, 0.017 6061, and 0.019 0614$k_BT/$nm for curves (1), (2), and (3), respectively. It is apparent that for ε_b distribution the longer WLCs will be wider. To accommodate larger string length on the same curved surface space, a WLC needs to make more turns as shown in Fig. 2(a). The left- and right-
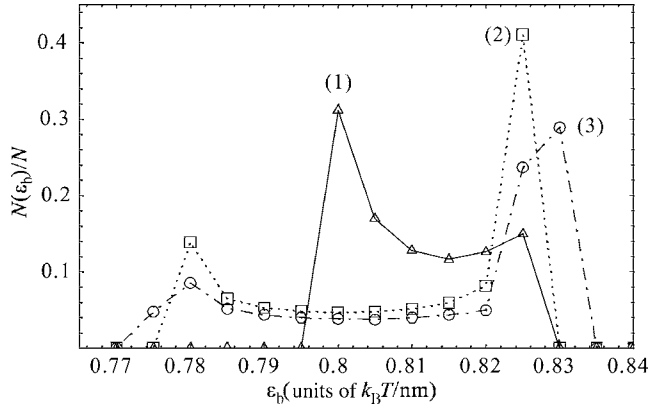
FIG. 3. Bending energy per unit length distribution diagram for curves in Fig. 2(b).

hand peaks in Fig. 3 correspond to the valley and peaks in Fig. 2(b), respectively.

It is of interest to know whether the studies presented above bear some relevance to the package of DNA in cells. A basic unit for the package of DNA in eucaryote cells is nucleosome. A nucleosome consists of a histone octamer core (pairs of H3, H4, H2A, and H2B), a DNA of 180–200 base pairs around the octamer core, and a linker histone (H1). For the DNA-histone octamer complex [16,17], H1 can bind to each nucleosome near the site where the DNA enters and leaves the histone octamer, and then plays the role of fixing both ends of the chain. In this case, it corresponds to the boundary value problem. Here we ignore the effects of fluctuations at the boundaries for the existence of H1 molecule might strengthen the attraction between the DNA and the protein core at the boundaries. However, recent evidence indicates the H1 molecule is situated asymmetrically, and it may be related to an initial value problem. Meanwhile, the initial and boundary value problem can also be relevant to the experiments for the single macromolecule (say DNA) attached to protein surface by the manipulation of optical tweezers on one or two endpoints, respectively [18].

Ellipsoidal surface. For simplicity, we consider the ellipsoid with two equal semiaxis lengths. Then, an ellipsoidal (or spheroidal) surface could be parametrized as $\mathbf{r}=(a\sin\theta\cos\phi, a\sin\theta\sin\phi, b\cos\theta)$, $0\leqslant\theta\leqslant\pi$, $0\leqslant\phi<2\pi$, where a and b are semiaxis lengths of an ellipsoid in the x (or y) and z directions, respectively. The conformation of a polymer on this surface can be described by

$$\mathbf{r}(\theta(s),\phi(s))$$
$$= (a\sin\theta(s)\cos\phi(s), a\sin\theta(s)\sin\phi(s), b\cos\theta(s)).$$

The constraint of Eq. (21) can be recast into the following form:

$$[a^2+b^2+(a^2-b^2)\cos 2\theta(s)][\theta'(s)]^2 + 2a^2\sin^2\theta(s)[\phi'(s)]^2$$
$$= 2. \tag{23}$$

Here a and b are taken as 5.5 and 6 nm, respectively. A schematic draw of three WLCs wrapping around an ellipsoidal surface is shown in Fig. 1(b), whose boundary conditions will be given in the following paragraph.
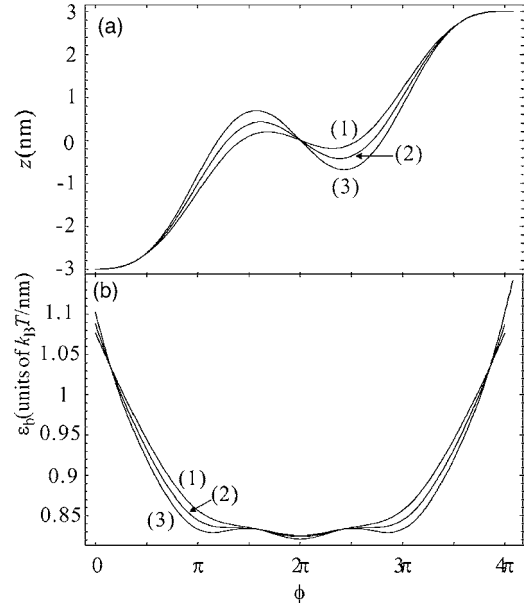

FIG. 4. Conformations of a WLC wrapping around an ellipsoidal surface with two identical endpoints: (a) Dependence of z on ϕ. (b) Bending energy per unit length of a WLC versus ϕ. Their boundary conditions are $\theta'=0$ at both ends and their lengths are 66.377, 66.595, and 66.790 nm, respectively.

Figure 4(a) shows the dependence of z on ϕ for three conformations of a WLC wrapping around an ellipsoidal surface. Here curves (1), (2), and (3) correspond to the red, green, and blue curves in Fig. 1(b), respectively. The coordinates of the endpoints are $(\theta,\phi)=(\cos^{-1}(-3/b),0)$ and $(\cos^{-1}(3/b),4\pi)$ for $s=0$ and L, respectively. The boundary conditions at both ends are $\theta'(0)=\theta'(L)=0$, and the contour lengths are 66.377, 66.595, and 66.790 nm for curves (1), (2), and (3), respectively.

In Fig. 4(b), we show the bending energy per unit length, ε_b, versus the azimuthal angle ϕ, respectively, for three conformations in Fig. 4(a). We note that ε_b is higher near $\phi=0$ and $\phi=4\pi$ for all curves and therefore the WLCs are attached weakly at the anchored point and are prone to be detached from the surface. In general, the elasticity energy per unit length near the middle of the chain is lower than that at both ends. This fact can be accounted for by the small curvature near the belly of the ellipsoid. Thus energy cost for bending of a WLC is lower and the WLC can wrap more tightly around the surface belly. From the free energy distribution with respect to positions, it is energetically favorable to dewrap the WLC from the surface at both ends than in the middle of the chain. However, this behavior is very different from that of the cylindrical case. For the cylindrical case, the values of ε_b oscillate between a minimum and a maximum. The maximum ε_b value appears periodically but not on the endpoint of the WLC in contrast to the ellipsoidal case.

Figure 5 shows ε_b distribution corresponding to curves in Fig. 4(b). Here the values of N and $\Delta\varepsilon_b$ are equal to 5000 and $0.01k_BT/$nm, respectively. The maximum probability of ε_b occurs at lower ε_b (about 0.83) related to the bending energy per unit length around the belly. The standard deviations for the data are calculated as 0.072 2204, 0.072 5575,
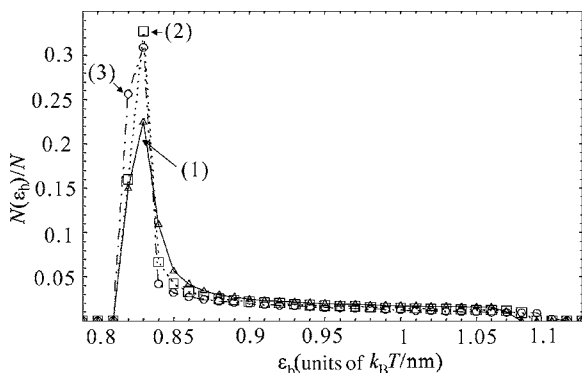
FIG. 5. Bending energy per unit length distribution diagram for curves in Fig. 4(b).

and $0.073\,735 k_B T/\mathrm{nm}$ for curves (1), (2), and (3), respectively. Again, the longer WLC comes with wider ε_b distribution and this result is similar to that of the cylindrical case.

We coin the term "threshold wrapping length" L_{th}, which is the length between two positions with elasticity energy per unit length overcoming the attraction energy per unit length. On an ellipsoidal surface, the curvature of a WLC wrapping in ϕ direction and bending energy increases toward the north and south poles of the ellipsoid. The wrapping of a WLC near the poles usually requires very high elasticity energy, and then segments prefer to detach from the surface.

Figure 6 shows the dependence of the threshold wrapping length L_{th} on the anchored position θ (initial position) along a meridian line on the ellipsoidal surface with various D values. For a WLC wrapping one to two revolutions from $z=-3$ to $z=3$ (like DNA-histone octomer complex), its average θ' value is roughly estimated from -0.015 to -0.03.
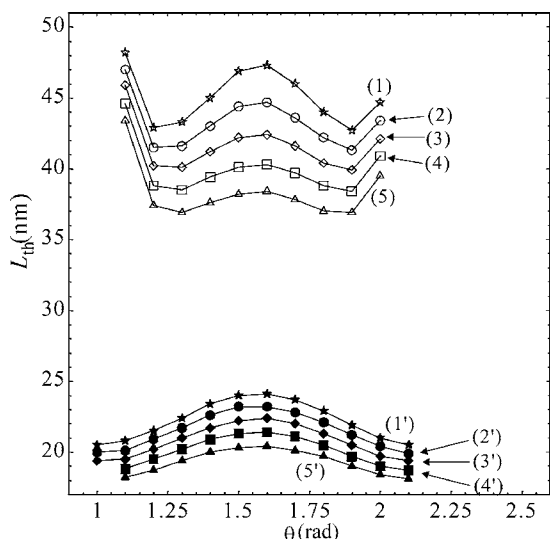

FIG. 6. Dependence of threshold dewrapping length L_{th} on the initially anchored position θ along a meridian line for (1), (1')$D=-1.2$, (2), (2')$D=-1.175$, (3), (3')$D=-1.15$, (4), (4')$D=-1.125$, and (5), (5')$D=-1.1 k_B T/\mathrm{nm}$. Here the initial conditions for curves (1)–(5) are taken as $\theta'=-0.03$ and $\theta''=\theta^{(3)}=\theta^{(4)}$ $=0$. As for curves (1')–(5'), we only change $\theta^{(3)}$ values in the above from 0 to -0.001.
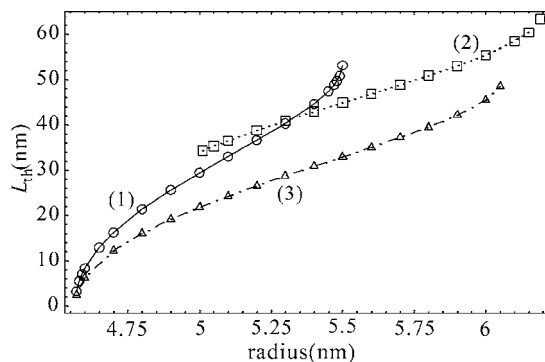

FIG. 7. Wrapping length L_{th} versus the radius of a sphere core. The initial values of (θ,θ') are $(1.57,-0.03)$, $(2,-0.03)$, and $(1.57,-0.04)$ for curves (1), (2), and (3), respectively. Besides, θ'', $\theta^{(3)}$, and $\theta^{(4)}$ are set to be none at the anchored point for all curves.

Hence, we take the initial conditions as $\theta'=-0.03$, and $\theta''=\theta^{(3)}=\theta^{(4)}=0$ for curves from (1) to (5); i.e., the tangent vector of the WLC at the anchored position is given. Then the WLC shoots in both forward and backward directions until its ε_b reaches the value larger than the electrostatic attraction per unit length $|D|$. The values of D are -1.2, -1.175, -1.15, -1.125, and $-1.1 k_B T/\mathrm{nm}$ for curves (1), (2), (3), (4), and (5), respectively. Along a meridian we calculate several L_{th}'s for polymers with anchored points separated by 0.1 radian interval. All curves display a "W" shape. Valid threshold length values are found between $\theta=1.1$ and $\theta=2$. On the left-hand side for curves (1)–(3), the WLC intersects itself at $\theta=1$ and then ε_b overcomes $|D|$ for $\theta\leqslant 0.9$, but for curves (4) and (5), ε_b overcomes $|D|$ for $\theta\leqslant 1$ and no self-intersection occurs. On the right-hand side for all curves self-intersection occurs at $\theta=2.1$ and $\varepsilon_b\geqslant|D|$ for $\theta\geqslant 2.2$. Self-intersection configuration is not physically allowed and will be excluded, since the self-avoiding energy is not considered here. Polymers with different initial conditions should display different behaviors. When we change $\theta^{(3)}$ of the above initial conditions from zero to -0.001, we obtain curves (1')–(5'). The valid L_{th} are obtained between $\theta=1$ and $\theta=2.1$ for curves (1')–(3') and between $\theta=1.1$ and $\theta=2.1$ for curves (4') and (5'). Beyond the valid range, ε_b overcomes $|D|$. There is no self-intersection occurred. Our investigation reveals that one had better set the anchored point near the belly of the ellipsoid; otherwise, the WLC will intersect itself or detach from the ellipsoidal surface easily. When $|D|$ decreases, curves move toward the θ axis. The L_{th} is decreasing with $|D|$, whose values can be varied by controlling salt concentrations. At high salt concentrations, DNA-core attractions become weaker and result in smaller values of $|D|$ and hence L_{th} (Fig. 6). In such cases, the DNA dewraps more easily from the surface of histone core, which is in qualitative agreement with experimental data [7].

For the case of a sphere with $a=b$, the dependence of L_{th} on the radius is shown in Fig. 7. The initial values of (θ,θ') are $(1.57,-0.03)$, $(2,-0.03)$, and $(1.57,-0.04)$ for curves (1), (2), and (3), respectively. Besides, θ'', $\theta^{(3)}$, and $\theta^{(4)}$ are set to be zero at the anchored point for all curves. Here D is equal to $-1.2 k_B T/\mathrm{nm}$. The threshold length L_{th} increases with the radius in a finite range for all curves. It is intuitive that this

trend is qualitatively universal for any fixed initial condition and here we provide quantitative results. Such a finite allowed range due to the exclusion of self-intersection cannot be found by a simple way and is determined by the conditions of the anchored point. When the core radius is larger than a certain value, 5.5, 6.19, and 6.05 nm for curves (1), (2), and (3), respectively, the WLC will intersect itself. For the radius smaller than 4.57, 5.01, and 4.57 nm for curves (1), (2), and (3), respectively, ε_b will be too large to wrap the core.

IV. DISCUSSION

To conclude, we find that a WLC usually has various elasticity energies per unit length at different positions. It may be due to the uniform curvature of a cylindrical surface, the ε_b oscillates almost periodically between a maximum and a minimum value. The ε_b value of WLCs on a cylindrical surface has a tendency to be spatially uniform. The variation of ε_b is much smaller than that in the ellipsoidal cases. The probability for dewrapping a polymer from a core at any position is almost equal, thus there is no particular position for the WLC to be detached from the cylindrical surface easily.

However, a WLC will detach from an ellipsoidal surface beyond the threshold wrapping length. A WLC wrapping around an ellipsoidal surface usually has higher elasticity energy near the pole and the dewrapping occurs. One expects that the wrapping-dewrapping transition can occur by the controls of salt concentration. In agreement with experiments, for high salt the weakening of DNA-core attraction induces dewrapping [7].

The position of initially anchored point of a polymer on the core surface will have a significant effect on its conformation and threshold length. Figure 6 provides some examples. Our investigation shows that the polymer with longer threshold length should initially contact the surface near the belly region. Otherwise, the polymer will not wrap the core successfully for high bending energy or be led to intersect itself.

We note in passing that L_{th} increases monotonically with the radius of a sphere core but it will not extend to infinity. For a larger radius, the L_{th} goes longer and the WLC may suffer from intersecting itself. For a small radius, the bending energy will be large enough to overcome the electrostatic attraction between the WLC and the core and lead to dewrapping. Hence, we expect that there is an optimum radius for the stability of DNA-histone complex, whose prediction is beyond the scope of this paper.

Although we present applications of the governing equations to cylinder- and ellipsoid-shaped surfaces in this work, derived equations are quite general and can be adopted to investigate nanoparticles with some other shapes, such as oblate or prolate surfaces. Meanwhile, our approach should be also applicable to the issue of the dynamics of polymer chain on a nanoparticle surface. In spite of curvature $\kappa(s)$, the torsion term, $\tau(s)$, is also needed to describe a space curve. The helix-free polymer energy may depend on the torsion. It is reasonable to express its related energy in a

similar form as the bending energy. The details are referred to Appendix C. Segment-segment interactions within a polymer chain should exert some effects on its conformation, which are neglected in this work. We will leave them as a future work.

Very recently, Allahverdyan *et al.* studied the adhesion of double-stranded DNA on the flat surface [19]. In such a study, interstrand potential between two strands of DNA has been taken into account. It is of interest to combine some ideas from the approach by Allahverdyan *et al.* and the approach of the present paper to study the adhesion of double-stranded DNA on curved surfaces.

APPENDIX A: GEODESIC CURVE

In this Appendix, we will take the classic example, a geodesic on a surface to expound the method used in Sec. II. The present method has the advantage that the derived equations are expressed in terms of geometrical quantities such as $\kappa(s)$, $\tau(s)$, and $\mathbf{T}(s),\dots$. Suppose S is a C^∞ curved surface where C^∞ means the position vector of S is differentiable to infinite order. The position vector of a point on the surface S can be expressed as $\mathbf{r}(u_1,u_2)=(x(u_1,u_2),y(u_1,u_2),z(u_1,u_2))$. Consider a curve C lying on S with A and B as its initial and final endpoints parametrized by $u_1=u_1(s)$ and $u_2=u_2(s)$, where s is the arc-length of the curve C. The position vector of C is expressed as $\mathbf{r}(u_1(s),u_2(s))=\mathbf{r}(s)$, its unit tangential vector is $\mathbf{T}(s)=d\mathbf{r}(s)/ds$, and its unit normal vector on S along C is $\mathbf{n}(s)$.

We consider a family of curves C_λ with A and B as two fixed endpoints as parametrized in Eq. (8). As λ is fixed, $\mathbf{r}(u_1(s,\lambda),u_2(s,\lambda))$ represents a curve C_λ from A to B. When $\lambda\neq 0$, s is not the arc-length parameter of C_λ.

Apparently, the tangent vectors $\mathbf{T}(s)$ is given by

$$\frac{d\mathbf{r}(s)}{ds}=\mathbf{T}(s)=\left.\frac{\partial\mathbf{r}(u_1(s,\lambda),u_2(s,\lambda))}{\partial s}\right|_{\lambda=0}$$

$$=\frac{d\mathbf{r}(u_1(s,0),u_2(s,0))}{ds}=\frac{d\mathbf{r}(u_1(s),u_2(s))}{ds}. \quad \text{(A1)}$$

When s is kept fixed and λ is varied, we derive another family of curve C_s^*. Its tangential vector is $\partial\mathbf{r}(u_1(s,\lambda),u_2(s,\lambda))/\partial\lambda$. When λ is null, we define the variational vector $\mathbf{J}(s)$ as Eq. (9). The variational vector $\mathbf{J}(s)$ is decomposed into two components as in Eq. (10).

Along the curve C_λ with fixed λ, the contour length from A to B is

$$L(C_\lambda) = \int_a^b \left| \frac{\partial \mathbf{r}}{\partial s} \right| ds = \int_a^b \sqrt{\frac{\partial \mathbf{r}}{\partial s} \cdot \frac{\partial \mathbf{r}}{\partial s}} ds, \quad \text{(A2)}$$

where

$$\frac{\partial \mathbf{r}}{\partial s} = \frac{\partial \mathbf{r}(u_1(s,\lambda), u_2(s,\lambda))}{\partial s}. \quad \text{(A3)}$$

Its derivative with respect to λ can be rewritten as

$$\frac{dL(C_\lambda)}{d\lambda} = \int_a^b \frac{\partial}{\partial \lambda} \sqrt{\frac{\partial \mathbf{r}}{\partial s} \cdot \frac{\partial \mathbf{r}}{\partial s}} ds = \int_a^b \frac{\frac{\partial}{\partial \lambda} \left(\frac{\partial \mathbf{r}}{\partial s} \cdot \frac{\partial \mathbf{r}}{\partial s} \right)}{2\sqrt{\frac{\partial \mathbf{r}}{\partial s} \cdot \frac{\partial \mathbf{r}}{\partial s}}} ds$$

$$= \int_a^b \frac{\frac{\partial^2 \mathbf{r}}{\partial s \partial \lambda} \cdot \frac{\partial \mathbf{r}}{\partial s}}{\sqrt{\frac{\partial \mathbf{r}}{\partial s} \cdot \frac{\partial \mathbf{r}}{\partial s}}} ds. \quad \text{(A4)}$$

From Eqs. (A1) and (9), we have

$$\mathbf{T}(s) \cdot \mathbf{T}(s) = 1, \quad \text{(A5)}$$

and

$$\left. \frac{\partial^2 \mathbf{r}(s)}{\partial s \partial \lambda} \right|_{\lambda=0} = \frac{d\mathbf{J}(s)}{ds}. \quad \text{(A6)}$$

Substituting Eqs. (A1), (A5), and (A6), into (A4) yields

$$\left. \frac{dL(C_\lambda)}{d\lambda} \right|_{\lambda=0} = \int_a^b \frac{d\mathbf{J}(s)}{ds} \cdot \mathbf{T}(s) ds, \quad \text{(A7)}$$

where a and b are the values of s at the endpoints. The further simplification of Eq. (A7) can be proceeded by writing $d\mathbf{J}/ds$ as

$$\frac{d\mathbf{J}(s)}{ds} = \frac{d}{ds}[l(s)\mathbf{T}(s) + h(s)\mathbf{n}(s) \times \mathbf{T}(s)] = \frac{ds(s)}{ds}\mathbf{T}(s)$$

$$+ l(s)\kappa(s)\mathbf{N}(s) + \frac{dh(s)}{ds}\mathbf{n}(s) \times \mathbf{T}(s) + h(s)\frac{d\mathbf{n}(s)}{ds}$$

$$\times \mathbf{T}(s) + h(s)\mathbf{n}(s) \times \frac{d\mathbf{T}(s)}{ds}, \quad \text{(A8)}$$

where Eq. (10) is used for the derivation. From Eqs. (4) and (6), it is easy to obtain the identities as follows:

$$\mathbf{N}(s) \cdot \mathbf{T}(s) = 0,$$

$$[\mathbf{n}(s) \times \mathbf{T}(s)] \cdot \mathbf{T}(s) = 0,$$

$$\left[\frac{d\mathbf{n}(s)}{ds} \times \mathbf{T}(s) \right] \cdot \mathbf{T}(s) = 0. \quad \text{(A9)}$$

The contribution from each term in Eq. (A9) to the right-hand side of Eq. (A8) is null. Combining Eqs. (5) with (7), we also have

$$\frac{d\mathbf{T}(s)}{ds} = \kappa(s)\mathbf{N}(s) = \kappa_g(s)[\mathbf{n}(s) \times \mathbf{T}(s)] + \kappa_n(s)\mathbf{n}(s),$$

$$\text{(A10)}$$

and thus

$$\mathbf{n}(s) \times \frac{d\mathbf{T}(s)}{ds} = \kappa_g(s)\mathbf{n}(s) \times [\mathbf{n}(s) \times \mathbf{T}(s)]$$

$$= \kappa_g(s)\{[\mathbf{T}(s) \cdot \mathbf{n}(s)]\mathbf{n}(s) - [\mathbf{n}(s) \cdot \mathbf{n}(s)]\mathbf{T}(s)\}$$

$$= -\kappa_g(s)\mathbf{T}(s). \quad \text{(A11)}$$

By using Eqs. (A8), (A9), and (A11), we obtain

$$\frac{d\mathbf{J}(s)}{ds} \cdot \mathbf{T}(s) = \frac{dl(s)}{ds} - h(s)\kappa_g(s). \quad \text{(A12)}$$

The substitution of Eq. (A12) into Eq. (A7) gives

$$\left. \frac{dL(C_\lambda)}{d\lambda} \right|_{\lambda=0} = \int_a^b \left(\frac{dl(s)}{ds} - h(s)\kappa_g(s) \right) ds$$

$$= [l(b) - l(a)] - \int_a^b h(s)\kappa_g(s) ds.$$

$$\text{(A13)}$$

Because of $l(a) = l(b) = 0$, we obtain

$$\left. \frac{dL(C_\lambda)}{d\lambda} \right|_{\lambda=0} = -\int_a^b h(s)\kappa_g(s) ds. \quad \text{(A14)}$$

For a curve C on a curved surface, the sufficient condition for C to be a geodesic is the contour length of C to be a minimum, i.e., $dL(C_\lambda)/d\lambda|_{\lambda=0} = 0$. Finally, we arrive at the known condition, $\kappa_g(s) = 0$, for a geodesic curve C [13].

APPENDIX B: DERIVATION OF GOVERNING EQUATIONS IN DETAILS

In this Appendix, we will present the detailed derivation of Eq. (15). Starting from Eq. (15) and combining Eqs. (2) with (A2), we have

$$\frac{\partial H_{\text{ben}}}{\partial \lambda} = \frac{A}{2} \int_{C_\lambda} \left(\frac{\partial \kappa^2}{\partial \lambda} \sqrt{\frac{\partial \mathbf{r}}{\partial s} \cdot \frac{\partial \mathbf{r}}{\partial s}} + \kappa^2 \frac{\partial}{\partial \lambda} \sqrt{\frac{\partial \mathbf{r}}{\partial s} \cdot \frac{\partial \mathbf{r}}{\partial s}} \right) ds.$$

$$\text{(B1)}$$

With

$$\kappa^2|_{\lambda=0} = \left(\frac{d\mathbf{T}(s)}{ds} \right)^2 \quad \text{(B2)}$$

and

$$\left. \frac{\partial^2 \mathbf{T}}{\partial s \partial \lambda} \right|_{\lambda=0} = \frac{d^2\mathbf{J}(s)}{ds^2}, \quad \text{(B3)}$$

Eq. (B1) can be expressed as

$$\frac{\partial H_{\text{ben}}}{\partial \lambda}\bigg|_{\lambda=0} = \frac{A}{2}\int_{C_\lambda} \left(2\frac{d^2\mathbf{J}(s)}{ds^2}\cdot\frac{d\mathbf{T}(s)}{ds}\right.$$

$$\left. + \kappa(s)^2\frac{d\mathbf{J}(s)}{ds}\cdot\mathbf{T}(s)\right)ds\bigg|_{\lambda=0}. \qquad \text{(B4)}$$

The term $d^2\mathbf{J}(s)/d^2s$ can be calculated straightforwardly as

$$\frac{d^2\mathbf{J}(s)}{ds^2} = \frac{d^2l(s)}{ds^2}\mathbf{T}(s) + \frac{dl(s)}{ds}\frac{d\mathbf{T}(s)}{ds} + \frac{d[l(s)\kappa(s)]}{ds}\mathbf{N}(s)$$

$$+ l(s)\kappa(s)\frac{d\mathbf{N}(s)}{ds} + \frac{d^2h(s)}{ds^2}[\mathbf{n}(s)\times\mathbf{T}(s)]$$

$$+ 2\frac{dh(s)}{ds}\left(\frac{d\mathbf{n}(s)}{ds}\times\mathbf{T}(s)\right) + \frac{dh(s)}{ds}\left(\mathbf{n}(s)\times\frac{d\mathbf{T}(s)}{ds}\right)$$

$$+ h(s)\left(\frac{d^2\mathbf{n}(s)}{ds^2}\times\mathbf{T}(s)\right) + h(s)\left(\frac{d\mathbf{n}(s)}{ds}\times\frac{d\mathbf{T}(s)}{ds}\right)$$

$$- \frac{d[h(s)\kappa_g(s)]}{ds}\mathbf{T}(s) - h(s)\kappa_g(s)\frac{d\mathbf{T}(s)}{ds}, \qquad \text{(B5)}$$

by differentiating Eq. (A8) one time. From Eqs. (4), (6), (5), and (A10), one can easily obtain the following identities:

$$\mathbf{T}(s)\cdot\frac{d\mathbf{T}(s)}{ds} = 0, \quad \frac{d\mathbf{T}(s)}{ds}\cdot\frac{d\mathbf{T}(s)}{ds} = \kappa(s)^2,$$

$$\mathbf{N}(s)\cdot\frac{d\mathbf{T}(s)}{ds} = \kappa(s),$$

$$\frac{d\mathbf{N}(s)}{ds}\cdot\frac{d\mathbf{T}(s)}{ds} = 0, \quad [\mathbf{n}(s)\times\mathbf{T}(s)]\cdot\frac{d\mathbf{T}(s)}{ds} = \kappa_g(s),$$

$$\left(\frac{d\mathbf{n}(s)}{ds}\times\mathbf{T}(s)\right)\cdot\frac{d\mathbf{T}(s)}{ds} = \kappa_n(s)\frac{d\mathbf{n}(s)}{ds}\cdot[\mathbf{T}(s)\times\mathbf{n}(s)],$$

$$\left(\mathbf{n}(s)\times\frac{d\mathbf{T}(s)}{ds}\right)\cdot\frac{d\mathbf{T}(s)}{ds} = 0,$$

$$\left(\frac{d^2\mathbf{n}(s)}{ds^2}\times\mathbf{T}(s)\right)\cdot\frac{d\mathbf{T}(s)}{ds} = \kappa_g(s)\mathbf{n}(s)\cdot\frac{d^2\mathbf{n}(s)}{ds^2}$$

$$+ \kappa_n[\mathbf{T}(s)\times\mathbf{n}(s)]\cdot\frac{d^2\mathbf{n}(s)}{ds^2},$$

$$\left(\frac{d\mathbf{n}(s)}{ds}\times\frac{d\mathbf{T}(s)}{ds}\right)\cdot\frac{d\mathbf{T}(s)}{ds} = 0. \qquad \text{(B6)}$$

By employing Eq. (B6), we have

$$\frac{d^2\mathbf{J}(s)}{ds^2}\cdot\frac{d\mathbf{T}(s)}{ds} = \frac{dl(s)}{ds}2\kappa(s)^2 + l(s)\frac{d\kappa(s)}{ds}\kappa(s) + \frac{d^2h(s)}{ds^2}\kappa_g(s)$$

$$+ \frac{dh(s)}{ds}\left(2\kappa_n(s)\frac{d\mathbf{n}(s)}{ds}\cdot[\mathbf{T}(s)\times\mathbf{n}(s)]\right)$$

$$+ h(s)\left(\kappa_g(s)\mathbf{n}(s)\cdot\frac{d^2\mathbf{n}(s)}{ds^2} - \kappa_g(s)\kappa(s)^2\right.$$

$$+ \kappa_n(s)[\mathbf{T}(s)\times\mathbf{n}(s)]\cdot\frac{d^2\mathbf{n}(s)}{ds^2}\right). \qquad \text{(B7)}$$

The substitution of Eqs. (A12) and (B7) into Eq. (B4) gives

$$\frac{\partial H_{\text{ben}}}{\partial \lambda}\bigg|_{\lambda=0} = \frac{A}{2}\int_0^L \left[\frac{dl(s)}{ds}5\kappa(s)^2\right.$$

$$+ l(s)2\frac{d\kappa(s)}{ds}\kappa(s) + \frac{d^2h(s)}{ds^2}2\kappa_g(s)$$

$$+ \frac{dh(s)}{ds}\left(4\kappa_n(s)\frac{d\mathbf{n}(s)}{ds}\cdot[\mathbf{T}(s)\times\mathbf{n}(s)]\right)$$

$$+ h(s)\left(2\kappa_g(s)\mathbf{n}(s)\cdot\frac{d^2\mathbf{n}(s)}{ds^2} - 3\kappa_g(s)\kappa(s)^2\right.$$

$$\left.\left. + 2\kappa_n(s)[\mathbf{T}(s)\times\mathbf{n}(s)]\cdot\frac{d^2\mathbf{n}(s)}{ds^2}\right)\right]ds. \qquad \text{(B8)}$$

Integration by parts for the derivative terms of $l(s)$ and $h(s)$ in Eq. (B8) gives

$$\int_0^L \frac{dl(s)}{ds}[5\kappa(s)^2]ds = 5\kappa(s)^2l(s)\big|_0^L - \int_0^L l(s)$$

$$\times\left(10\kappa(s)\frac{d\kappa(s)}{ds}\right)ds, \qquad \text{(B9)}$$

$$\int_0^L \frac{d^2h(s)}{ds^2}[2\kappa_g(s)]ds = \left(2\kappa_g(s)\frac{dh(s)}{ds} - 2\frac{d\kappa_g(s)}{ds}h(s)\right)\bigg|_0^L$$

$$+ \int_0^L h(s)\left(2\frac{d^2\kappa_g(s)}{ds^2}\right)ds, \qquad \text{(B10)}$$

and

$$\int_0^L \frac{dh(s)}{ds}\left(4\kappa_n(s)\frac{d\mathbf{n}(s)}{ds}\cdot[\mathbf{T}(s)\times\mathbf{n}(s)]\right)ds$$

$$= h(s)\left(4\kappa_n(s)\frac{d\mathbf{n}(s)}{ds}\cdot[\mathbf{T}(s)\times\mathbf{n}(s)]\right)\bigg|_0^L$$

$$- \int_0^L h(s)\frac{d}{ds}\left(4\kappa_n(s)\frac{d\mathbf{n}(s)}{ds}\cdot[\mathbf{T}(s)\times\mathbf{n}(s)]\right)ds. \qquad \text{(B11)}$$

Assume the values of $l(s)$, $h(s)$, and $dh(s)/ds$, which result in the required boundary condition at both endpoints, vanish. The substitution of Eqs. (B9)–(B11) into Eq. (B8) yields Eq. (15).

APPENDIX C: AN ADDITIONAL CORRECTION TERM— TORSIONAL ENERGY

In this Appendix, we demonstrate to add an energy term to Eq. (1) only for academic interest. According to the fundamental theorem of a space curve [13], its conformation can be uniquely determined up to some rigid rotation or translation, by knowing its values of curvature and torsion at each

point. For a general consideration (other than DNA polymer case), elastic energy of a string may depend on the torsion. We intend to calculate the energy related to the geometrical torsion. In geometry,

$$\mathbf{B}(s) = \mathbf{T}(s) \times \mathbf{N}(s), \tag{C1}$$

Eqs. (4) and (6) form three mutually normal vectors at a point s. They are related to each other via Frenet formulas [13,20]. To characterize the feature of a space curve at a point s, one may also introduce the changes of the triple unit vectors with respect to the chain length. The derivative of $\mathbf{T}(s)$ is shown in Eq. (5) and those of $\mathbf{N}(s)$ and $\mathbf{B}(s)$ take the forms of

$$\frac{d\mathbf{N}(s)}{ds} = -\kappa(s)\mathbf{T}(s) - \tau(s)\mathbf{B}(s), \tag{C2}$$

$$\frac{d\mathbf{B}(s)}{ds} = \tau(s)\mathbf{N}(s), \tag{C3}$$

where $\kappa(s)$ and $\tau(s)$ are the curvature and torsion of a space curve at s. By observing Eqs. (5), (C2), and (C3), we find $\kappa(s)$ and $\tau(s)$ play very like actors. Therefore, the torsional energy, H_{tor}, should have very similar form of H_{ben},

$$H_{\text{tor}} = \frac{C}{2} \int_0^L \tau^2(s) ds. \tag{C4}$$

Following the same fashion of obtaining Eq. (15), apart from the more complicated calculation. Taking the derivative of Eq. (C4) with respect to λ we have

$$\frac{\partial H_{\text{tor}}}{\partial \lambda} = \frac{C}{2} \int_{C_\lambda} \left(\frac{\partial \tau^2}{\partial \lambda} \sqrt{\frac{\partial \mathbf{r}}{\partial s} \cdot \frac{\partial \mathbf{r}}{\partial s}} + \tau^2 \frac{\partial}{\partial \lambda} \sqrt{\frac{\partial \mathbf{r}}{\partial s} \cdot \frac{\partial \mathbf{r}}{\partial s}} \right) ds. \tag{C5}$$

Taking λ to be null, the torsion square can be rewritten as

$$\tau^2|_{\lambda=0} = \left(\frac{d\mathbf{B}(s)}{ds} \right)^2, \tag{C6}$$

and by using Eq. (C1), we obtain

$$\frac{\partial \tau^2}{\partial \lambda} \bigg|_{\lambda=0} = \frac{\partial}{\partial \lambda} \left(\frac{\partial \mathbf{B}}{\partial s} \right)^2 \bigg|_{\lambda=0}$$

$$= 2 \frac{\partial \mathbf{B}}{\partial s} \cdot \left(\frac{\partial^2 \mathbf{T}}{\partial \lambda \partial s} \times \mathbf{N} + \frac{\partial \mathbf{T}}{\partial s} \times \frac{\partial \mathbf{N}}{\partial \lambda} \right.$$

$$\left. + \frac{\partial \mathbf{T}}{\partial \lambda} \times \frac{\partial \mathbf{N}}{\partial s} + \mathbf{T} \times \frac{\partial^2 \mathbf{N}}{\partial \lambda \partial s} \right) \bigg|_{\lambda=0}. \tag{C7}$$

By using Eqs. (5) and (9), we can express the terms $\partial \mathbf{N}/\partial \lambda$ and $\partial^2 \mathbf{N}/\partial \lambda \partial s$ at $\lambda=0$ as

$$\frac{\partial \mathbf{N}}{\partial \lambda} \bigg|_{\lambda=0} = -\frac{1}{\kappa(s)^2} \left(\mathbf{N}(s) \cdot \frac{d^2 \mathbf{J}(s)}{ds^2} \right) \frac{d\mathbf{T}(s)}{ds} + \frac{1}{\kappa(s)} \frac{d^2 \mathbf{J}(s)}{ds^2}, \tag{C8}$$

and

$$\frac{\partial^2 \mathbf{N}}{\partial \lambda \partial s} \bigg|_{\lambda=0} = \frac{2}{\kappa(s)^3} \frac{d\kappa(s)}{ds} \left(\mathbf{N}(s) \cdot \frac{d^2 \mathbf{J}(s)}{ds^2} \right) \frac{d\mathbf{T}(s)}{ds}$$

$$- \frac{1}{\kappa(s)^2} \left(\frac{d\mathbf{N}(s)}{ds} \cdot \frac{d^2 \mathbf{J}(s)}{ds^2} + \mathbf{N}(s) \cdot \frac{d^3 \mathbf{J}(s)}{ds^3} \right) \frac{d\mathbf{T}(s)}{ds}$$

$$- \frac{1}{\kappa(s)^2} \left(\mathbf{N}(s) \cdot \frac{d^2 \mathbf{J}(s)}{ds^2} \right) \frac{d^2 \mathbf{T}(s)}{ds^2}$$

$$- \frac{1}{\kappa(s)^2} \frac{d\kappa(s)}{ds} \frac{d^2 \mathbf{J}(s)}{ds^2} + \frac{1}{\kappa(s)} \frac{d^3 \mathbf{J}(s)}{ds^3}. \tag{C9}$$

The substitution of Eqs. (C7)–(C9) into Eq. (C5) yields

$$\frac{\partial H_{\text{tor}}}{\partial \lambda} \bigg|_{\lambda=0} = C \int_0^L \tau(s) \mathbf{N}(s) \cdot \left[-\kappa(s) \frac{d\mathbf{J}(s)}{ds} \times \mathbf{T}(s) \right.$$

$$+ \frac{3}{2} \tau(s) \left(\frac{d\mathbf{J}(s)}{ds} \cdot \mathbf{T}(s) \right) \mathbf{N}(s)$$

$$- \frac{\tau(s)}{\kappa(s)} \left(\mathbf{N}(s) \cdot \frac{d^2 \mathbf{J}(s)}{ds^2} \right) \mathbf{N}(s) - \frac{1}{\kappa(s)^2} \frac{d\kappa(s)}{ds} \mathbf{T}(s)$$

$$\times \frac{d^2 \mathbf{J}(s)}{ds^2} + \frac{1}{\kappa(s)} \mathbf{T}(s) \times \frac{d^3 \mathbf{J}(s)}{ds^3} \right] ds. \tag{C10}$$

The simplification of Eq. (C10) is carried out by calculating the derivatives of $\mathbf{J}(s)$ to third order through Eq. (10). With Eqs. (C2) and (C1), it is useful to replace the $d\mathbf{N}(s)/ds$ and $\mathbf{B}(s)$ terms by $-\kappa(s)\mathbf{T}(s)-\tau(s)\mathbf{B}(s)$ and $\mathbf{T}(s) \times \mathbf{N}(s)$, respectively. The employment of the third term in Eq. (A9) and the following identities can be used to eliminate many terms with null contributions in Eq. (C10):

$$\mathbf{N}(s) \cdot [\mathbf{T}(s) \times \mathbf{T}(s)] = 0, \quad \mathbf{N}(s) \cdot [\mathbf{N}(s) \times \mathbf{T}(s)] = 0,$$

$$\mathbf{N}(s) \cdot \left(\frac{d\mathbf{T}(s)}{ds} \times \mathbf{T}(s) \right) = 0, \quad \mathbf{T}(s) \cdot \mathbf{n}(s) = 0. \tag{C11}$$

The following two identities are also handy in calculations:

$$\frac{d^2 \mathbf{T}(s)}{ds^2} = \frac{d}{ds}[\kappa(s)\mathbf{N}(s)] = \frac{d\kappa(s)}{ds}\mathbf{N}(s) + \kappa(s)\frac{d\mathbf{N}(s)}{ds}$$

$$= \frac{d\kappa(s)}{ds}\mathbf{N}(s) + \kappa(s)[-\kappa(s)\mathbf{T}(s) - \tau(s)\mathbf{B}(s)]$$

$$= \frac{d\kappa(s)}{ds}\mathbf{N}(s) - \kappa(s)^2 \mathbf{T}(s) - \kappa(s)\tau(s)[\mathbf{T}(s) \times \mathbf{N}(s)], \tag{C12}$$

$$\frac{d^2 \mathbf{N}(s)}{ds^2} = \frac{d}{ds}[-\kappa(s)\mathbf{T}(s) - \tau(s)\mathbf{B}(s)]$$

$$= -\frac{d\kappa(s)}{ds}\mathbf{T}(s) - [\kappa(s)^2 + \tau(s)^2]\mathbf{N}(s)$$

$$- \frac{d\tau(s)}{ds}[\mathbf{T}(s) \times \mathbf{N}(s)]. \tag{C13}$$

After a straightforward and tedious calculation, Eq. (C10) can be rewritten as

$$\frac{\partial H_{\mathrm{tor}}}{\partial \lambda}\bigg|_{\lambda=0} = C \int_0^L \Bigg\{ \frac{dl(s)}{ds}\left(\frac{5}{2}\tau(s)^2\right) + l(s)\tau(s)\frac{d\tau(s)}{ds} + \frac{d^3h(s)}{ds^3}\frac{\tau(s)\kappa_n(s)}{\kappa(s)^2} + \frac{d^2h(s)}{ds^2}\bigg(-\frac{\tau(s)^2}{\kappa(s)^2}\kappa_g(s) - \frac{\tau(s)\kappa_n(s)}{\kappa(s)^3}\frac{d\kappa(s)}{ds}$$

$$+ \frac{3\tau(s)}{\kappa(s)}\mathbf{N}(s)\cdot\frac{d\mathbf{n}(s)}{ds}\bigg) + \frac{dh(s)}{ds}\bigg[-2\frac{\tau(s)^2}{\kappa(s)^2}\kappa_n(s)\frac{d\mathbf{n}(s)}{ds}\cdot[\mathbf{T}(s)\times\mathbf{n}(s)] - 2\frac{\tau(s)}{\kappa(s)^2}\frac{d\kappa(s)}{ds}\mathbf{N}(s)\cdot\frac{d\mathbf{n}(s)}{ds}$$

$$+ \frac{3\tau(s)}{\kappa(s)}\mathbf{N}(s)\cdot\frac{d^2\mathbf{n}(s)}{ds^2} - 4\tau(s)\bigg(\mathbf{T}(s)\cdot\frac{d\mathbf{n}(s)}{ds}\bigg)\bigg] + h(s)\bigg[-\frac{3}{2}\tau(s)^2\kappa_g(s) - \frac{\tau(s)^2}{\kappa(s)^2}\kappa_g(s)\mathbf{n}(s)\cdot\frac{d^2\mathbf{n}(s)}{ds^2} - \frac{\tau(s)^2}{\kappa(s)^2}\kappa_n(s)[\mathbf{T}(s)$$

$$\times\mathbf{n}(s)]\cdot\frac{d^2\mathbf{n}(s)}{ds^2} - \frac{\tau(s)}{\kappa(s)^2}\frac{d\kappa(s)}{ds}\mathbf{N}(s)\cdot\frac{d^2\mathbf{n}(s)}{ds^2} - 2\tau(s)\bigg(\mathbf{T}(s)\cdot\frac{d^2\mathbf{n}(s)}{ds^2}\bigg) + \frac{\tau(s)}{\kappa(s)}\mathbf{N}(s)\cdot\frac{d^3\mathbf{n}(s)}{ds^3}\bigg]\Bigg\}ds. \tag{C14}$$

Performing the integration by parts for the derivative terms of $l(s)$ and $h(s)$ in Eq. (C14) and setting $l(s)$, $h(s)$, $dh(s)/ds$, and $d^2h(s)/ds^2$ as null at both ends, we obtain

$$\frac{\partial H_{\mathrm{tor}}}{\partial \lambda}\bigg|_{\lambda=0} = C\int_0^L [l(s)(-4\tau'(s)\tau(s)) + h(s)Y(s)]ds, \tag{C15}$$

where

$$Y(s) = (-\tau\kappa_n\kappa^{-2})''' + (-\tau^2\kappa^{-2}\kappa_g - \tau\kappa^{-3}\kappa_n\kappa' + 3\tau\kappa^{-2}\mathbf{T}'\cdot\mathbf{n}')'' + [2\tau\kappa^{-3}\kappa'\mathbf{T}'\cdot\mathbf{n}' - 3\tau\kappa^{-2}\mathbf{T}'\cdot\mathbf{n}'' + 4\tau\mathbf{T}\cdot\mathbf{n}'$$
$$+ 2\tau^2\kappa^{-2}\kappa_n\mathbf{n}'\cdot(\mathbf{T}\times\mathbf{n})]' - \tau^2\kappa^{-2}\mathbf{n}''\cdot[\kappa_g\mathbf{n} + \kappa_n(\mathbf{T}\times\mathbf{n})] - 3\tau^2\kappa_g/2 - \tau\kappa^{-3}\kappa'\mathbf{T}'\cdot\mathbf{n}'' - 2\tau\mathbf{T}\cdot\mathbf{n}'' + \tau\kappa^{-2}\mathbf{T}'\cdot\mathbf{n}'''. \tag{C16}$$

We substitute Eq. (C15) into Eq. (11) and Eqs. (19) and (20) become

$$\gamma'(s) + 4A\kappa(s)\kappa'(s) + 4C\tau(s)\tau'(s) = 0, \tag{C17}$$

$$\frac{A}{2}X(s) + CY(s) - [\gamma(s) + D]\kappa_g(s) = 0. \tag{C18}$$

[1] C. R. Calladine and H. R. Drew, *Understanding DNA: The Molecule and How it Works*, 2nd ed. (Academic, London, 1997).

[2] O. Kratky and G. Porod, Recl. Trav. Chim. Pays-Bas **68**, 1106 (1949); M. Wadati and H. Tsuru, Physica D **21**, 213 (1986); J. F. Marko and E. D. Siggia, Macromolecules **27**, 981 (1994); Z. Wei, Zhou Haijun, and O. Y. Zhong-can, Phys. Rev. E **58**, 8040 (1998); I. Tobias, D. Swigon, and B. D. Coleman, Phys. Rev. E **61**, 747 (2000).

[3] J. F. Marko and E. D. Siggia, Phys. Rev. E **52**, 2912 (1995).

[4] A. Vologodskii, *Topology and Physics of Circular DNA* (CRC Press, Boca Raton, FL, 1992).

[5] T. Wallin and P. Linse, Langmuir **12**, 305 (1996); R. R. Netz and J.-F. Joanny, Macromolecules **32**, 9026 (1999).

[6] S. Stoll and P. Chodanowski, Macromolecules **35**, 9556 (2002).

[7] D. J. Clark and T. Kimura, J. Mol. Biol. **211**, 883 (1990); K. K. Kunze and R. R. Netz, Phys. Rev. Lett. **85**, 4389 (2000).

[8] A. J. Spakowitz and Z.-G. Wang, Phys. Rev. Lett. **91**, 166102 (2003).

[9] R. P. Mondescu and M. Muthukumar, Phys. Rev. E **57**, 4411 (1998).

[10] H. Schiessel, R. F. Bruinsma, and W. M. Gelbart, J. Chem. Phys. **115**, 7245 (2001).

[11] M. D. Barkley and B. H. Zimm, J. Chem. Phys. **70**, 2991 (1979); M. T. Record, Jr., *et al.*, Annu. Rev. Biochem. **50**, 997 (1981); D. Shore and R. L. Baldwin, J. Mol. Biol. **170**, 957 (1983); I. Ashikawa *et al.*, Biochemistry **22**, 6018 (1983).

[12] J. F. Marko, Phys. Rev. E **55**, 1758 (1997).

[13] J. J. Stoker, "Differential Geometry," in *Pure and Applied Mathematics*, edited by R. Courant, L. Bers, and J. J. Stoker (Wiley, New York, 1969), Vol. 20.

[14] Haijun Zhou, Yang Zhang, and Zhong-can Ou-Yang Phys. Rev. E **62**, 1045 (2000).

[15] R. L. Burden and J. D. Faires, *Numerical Analysis*, 6th ed. (Brooks/Cole, Pacific Grove, 1997).

[16] B. Alberts, A. Johnson, J. Lewis, M. Raff, K. Roberts, and P. Walter, *Molecular Biology of the Cell*, 4th ed. (Garland, New York, 2002).

[17] G. Karp, *Cell and Molecular Biology: Concepts and Experiments*, 3rd ed. (Wiley, New York, 2002).

[18] S. Chu, Science **253**, 861 (1991).

[19] A. E. Allahverdyan, Zh. S. Gevorkian, C.-K. Hu, and T. M. Nieuwenhuizen, Phys. Rev. Lett. **96**, 098302 (2006).

[20] Z. C. Ou-Yang, J.-X. Liu, and Y.-Z. Xie, *Geometric Methods in the Elastic Theory of Membranes in Liquid Crystal Phases* (World Scientific, Singapore, 1999).